Physics Letters B 728 (2014) 602–606

Contents lists available at ScienceDirect

Physics Letters B

www.elsevier.com/locate/physletb

Searching for intrinsic charm in the proton at the LHC

V.A. Bednyakov [a], M.A. Demichev [a], G.I. Lykasov [a], T. Stavreva [b,*], M. Stockton [c]

[a] Joint Institute for Nuclear Research, Dubna 141980, Moscow region, Russia
[b] Laboratoire de Physique Subatomique et de Cosmologie, UJF, CNRS/IN2P3, INPG, 53 avenue des Martyrs, 38026 Grenoble, France
[c] Department of Physics, McGill University, Montreal, QC, Canada

ARTICLE INFO

Article history:
Received 21 May 2013
Received in revised form 9 December 2013
Accepted 9 December 2013
Available online 16 December 2013
Editor: D.F. Geesaman

ABSTRACT

Despite rather long-term theoretical and experimental study, the hypothesis of the non-zero intrinsic (or valence-like) heavy quark component of the proton distribution functions has not yet been confirmed or rejected. The LHC with pp-collisions at $\sqrt{s} = 7$–14 TeV will obviously supply extra unique information concerning the above-mentioned component of the proton. To use the LHC potential, first of all, one should select the parton-level (sub)processes (and final-state signatures) that are the most sensitive to the intrinsic heavy quark contributions. To this end inclusive production of $c(b)$-jets accompanied by photons is considered. On the basis of performed theoretical study it is demonstrated that investigation of the intrinsic heavy quark contributions looks very promising at the LHC in processes like $pp \to \gamma + c(b) + X$.

1. Introduction

The Large Hadron Collider (LHC) opens up new and unique kinematical regions with high accuracy for the investigation of the structure of the proton, in particular for the study of the parton distribution functions (PDFs). It is well known that the precise knowledge of the PDFs is very essential for the verification of the Standard Model and the search for New Physics.

By definition, the PDF $f_a(x, \mu)$ is a function of the proton momentum fraction x carried by parton a (quark q or gluon g) at the momentum transfer scale μ. For small values of μ, corresponding to long distance scales less than $1/\mu_0$, the PDF currently cannot be calculated from the first principles of QCD [1]. At $\mu > \mu_0$ the $f_a(x, \mu)$ can be obtained by means of solving the perturbative QCD evolution equations (DGLAP) [2]. At $\mu < \mu_0$ some progress in calculation of the PDFs has been achieved within the lattice methods [1]. The unknown (input for the evolution) functions $f_a(x, \mu_0)$ usually can be found empirically from some "QCD global analysis" [3,4] of a large variety of data typically at $\mu > \mu_0$.

In general, almost all pp processes at LHC energies, including Higgs boson production, are sensitive to the charm $f_c(x, \mu)$ or bottom $f_b(x, \mu)$ PDFs. Nevertheless, within the global analysis the charm content of the proton at $\mu \sim \mu_c$ and the bottom at $\mu \sim \mu_b$ are both assumed to be negligible. Here μ_c and μ_b are typical energy scales relevant to the c- and b-quark QCD excitation in the proton. These heavy quark components arise in the proton only perturbatively with increases in the Q^2-scale through the gluon splitting in the DGLAP Q^2 evolution [2]. Direct measurement of open charm and open bottom production in deep inelastic processes (DIS) confirms the perturbative origin of heavy quark flavors [5]. However, modern descriptions of these experimental data are not sensitive enough to the above-mentioned perturbative sea heavy quark distributions at relatively large x values ($x > 0.1$).

Analyzing hadroproduction of so-called leading hadrons Brodsky et al. [6,7] (about thirty years ago) has assumed co-existing of *extrinsic* and *intrinsic* contributions to the quark–gluon structure of the proton. The *extrinsic* (or ordinary) quarks and gluons are generated on a short time scale associated with large-transverse-momentum processes. Their distribution functions satisfy the standard QCD evolution equations. The *intrinsic* quarks and gluons exist over a time scale which is independent of any probe momentum transfer. They can be associated with a bound-state (zero-momentum transfer regime) hadron dynamics and one believes they have a nonperturbative origin.

It was shown in [7] that the existence of *intrinsic* heavy quark pairs $c\bar{c}$, and $b\bar{b}$ within the proton state can be due to the virtue of gluon-exchange and vacuum-polarization graphs. On this basis, within the MIT bag model [8], the probability to find a five-quark component $|uudc\bar{c}\rangle$ bound within the nucleon bag is non-zero and can be about 1–2%.

* Corresponding author.
E-mail addresses: Vadim.Bednyakov@cern.ch (V.A. Bednyakov), Mikhail.Demichev@cern.ch (M.A. Demichev), gennady.lykasov@cern.ch (G.I. Lykasov), stavreva@lpsc.in2p3.fr (T. Stavreva), mark.stockton@cern.ch (M. Stockton).

0370-2693
http://dx.doi.org/10.1016/j.physletb.2013.12.031

Initially in [6,7] S. Brodsky and coauthors proposed the existence of the 5-quark state $|uudc\bar{c}\rangle$ in the proton. Later some other models were developed. One of them considered a quasi-two-body state $\bar{D}^0(u\bar{c})\bar{\Lambda}_c^+(udc)$ in the proton [9]. In order to not contradict the DIS HERA data the probability to find the intrinsic charm (IC) in the proton (the weight of the relevant Fock state in the proton) was found to be less than 3.5% [9–12]. The probability of finding an intrinsic bottom state (IB) in the proton is suppressed by a factor of $m_c^2/m_b^2 \simeq 0.1$ [13], where $m_c \simeq 1.3$ GeV and $m_b = 4.2$ GeV are the current masses of the charm and bottom quarks. Therefore, the experimental search for a possible IC signal in pp collisions at the LHC energies is more promising than the search for the IB contribution.

If the distributions of the intrinsic charm or bottom in the proton are hard enough and similar in the shape to the valence quark distributions (i.e. have valence-like form), then one expects the production of the charmed (bottom) mesons or charmed (bottom) baryons in the fragmentation region to be similar to the production of pions or nucleons (from the light quarks). However, the yield of this production depends on the probability to find intrinsic charm or bottom in the proton, but this amount looks too small. The PDFs that include the IC contribution in the proton have already been used in perturbative QCD calculations in [9–12].

The probability distribution for the 5-quark state ($|uudc\bar{c}\rangle$) in the light-cone description of the proton was first calculated in [6]. The general form for this distribution calculated within the light-cone dynamics in the so-called BHPS model [6,7] can be written as [11]

$$P(x_1,\ldots,x_5) = N_5\delta\left(1-\sum_{j=1}^{5}x_j\right)\left(m_p^2-\sum_{j=1}^{5}\frac{m_j^2}{x_j}\right)^{-2}, \qquad (1)$$

where x_j is the momentum fraction of the parton, m_j is its mass and m_p is the proton mass. Neglecting the light quark (u,d,s) masses and the proton mass in comparison to the c-quark mass and integrating (1) over $dx_1\cdots dx_4$ one can get the probability to find the intrinsic charm with momentum fraction x_5 in the proton [11]:

$$P(x_5) = \frac{1}{2}\tilde{N}_5 x_5^2\left[\frac{1}{3}(1-x_5)\left(1+10x_5+x_5^2\right) - 2x_5(1+x_5)\ln(x_5)\right], \qquad (2)$$

where $\tilde{N}_5 = N_5/m_{4,5}^4$, $m_{4,5} = m_c = m_{\bar{c}}$, the normalization constant N_5 determines some probability $w_{\rm IC}$ to find the Fock state $|uudc\bar{c}\rangle$ in the proton. Fig. 1 illustrates the IC contribution in comparison to the conventional sea charm quark distribution in the proton.

The solid line in Fig. 1 shows the standard perturbative sea charm density distribution $xc_{\rm rg}(x)$ (ordinary sea charm) in the proton from CTEQ6.6M [12] as a function of x at $Q^2 = 1000$ GeV^2. The dashed curve in Fig. 1 is the sum of the intrinsic charm density $xc_{\rm in}(x)$ from CTEQ6.6C2 BHPS with the IC probability $w_{\rm IC} = 3.5\%$ and $xc_{\rm rg}(x)$ at the same Q^2 [12]. One can see from Fig. 1 that the IC distribution (with $w_{\rm IC} = 3.5\%$) given by (2) has a rather visible enhancement at $x \sim 0.2$–0.5 and this distribution is much larger (by an order and more of magnitude) than the sea (ordinary) charm density distribution in the proton.

As a rule, the gluons and sea quarks play the key role in hard processes of open charm hadroproduction. Simultaneously, due to the nonperturbative *intrinsic* heavy quark components one can expect some excess of these heavy quark PDFs over the ordinary sea quark PDFs at $x > 0.1$. Therefore the existence of this intrinsic charm component can lead to some enhancement in the

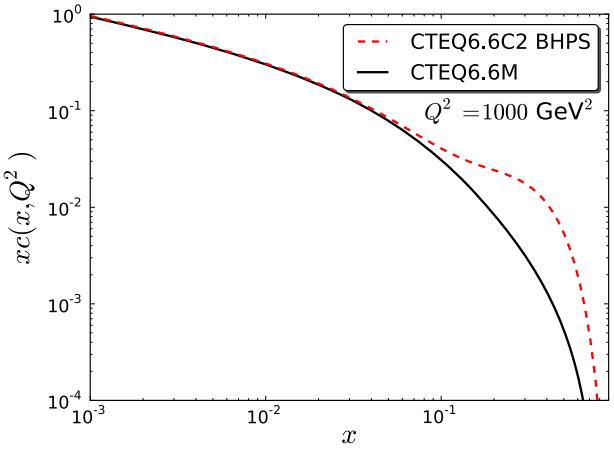

Fig. 1. Distributions of the charm quark in the proton at $Q^2 = 1000$ GeV^2. The solid line is the standard perturbative sea charm density distribution $xc_{\rm rg}(x)$ only, whereas the dashed curve is the charm quark distribution function, for the sum of the intrinsic charm density $xc_{\rm in}(x)$ (see (2)) and $xc_{\rm rg}(x)$.

inclusive spectra of open charm hadrons, in particular D-mesons, produced at the LHC in pp-collisions at large pseudorapidities η and large transverse momenta p_T [15]. Furthermore, as we know from [6–12] photons produced in association with heavy quarks Q ($\equiv c, b$) in the final state of pp-collisions provide valuable information about the parton distributions in the proton [9–23].

In this Letter, having in mind these considerations we will first discuss where the above-mentioned heavy flavor Fock states in the proton could be searched for at the LHC energies. Following this we analyze in detail, and give predictions for, the LHC semi-inclusive pp-production of prompt photons accompanied by c-jets including the *intrinsic* charm component in the PDF.

2. The intrinsic charm and beauty

According to the model of hard scattering [24–29] the relativistic invariant inclusive spectrum of the hard process $p+p \to h+X$ can be related to the elastic parton–parton subprocess $i+j \to i'+j'$, where i, j are the partons (quarks and gluons), by the formula [26,27]:

$$E\frac{d\sigma}{d^3p} = \sum_{i,j}\int d^2k_{iT}\int d^2k_{jT}\int_{x_i^{\min}}^{1}dx_i\int_{x_j^{\min}}^{1}dx_j\, f_i(x_i,k_{iT})\, f_j(x_j,k_{jT})\,\frac{d\sigma_{ij}(\hat{s},\hat{t})}{d\hat{t}}\,\frac{D_{i,j}^h(z_h)}{\pi z_h}. \qquad (3)$$

Here: $k_{i,j}$ and $k'_{i,j}$ are the four-momenta of the partons i or j before and after the elastic parton–parton scattering, respectively; k_{iT}, k_{jT} are the transverse momenta of the partons i and j; $f_{i,j}$ are the PDFs of partons i, j inside the proton; $D_{i,j}^h$ is the fragmentation function (FF) of the parton i or j to a hadron h; and z_h is the fraction of the final state hadron momentum from the parton momentum.

When the transverse momenta of the partons are neglected in comparison to the longitudinal momenta, the variables $\hat{s}$, $\hat{t}$, $\hat{u}$ and z_h can be presented in the following form [26]: $\hat{s} = x_i x_j s$, $\hat{t} = x_i\frac{t}{z_h}$, $\hat{u} = x_j\frac{u}{z_h}$, $z_h = \frac{x_1}{x_i}+\frac{x_2}{x_j}$, where, $x_1 = -\frac{u}{s} = \frac{x_T}{2}\cot(\theta/2)$, $x_2 = -\frac{t}{s} = \frac{x_T}{2}\tan(\theta/2)$, $x_T = 2\sqrt{tu}/s = 2p_T/\sqrt{s}$. Here as usual, $s = (p_1+p_2)^2$, $t = (p_1-p_1')^2$, $u = (p_2-p_1')^2$, and p_1, p_2, p_1' are the 4-momenta of the colliding protons and the produced hadron h, respectively; θ is the scattering angle of hadron h in the pp c.m.s. The lower

limits of the integration in (3) can be presented in the following form:

$$x_i^{\min} = \frac{x_R + x_F}{2 - (x_R - x_F)}, \qquad x_j^{\min} = \frac{x_i(x_R - x_F)}{2x_i - (x_R + x_F)}, \tag{4}$$

where $x_R = 2p/\sqrt{s}$ and the Feynman variable x_F of the produced hadron, for example the D-meson, can be expressed via the variables p_T and η, or θ being the hadron scattering angle in the pp c.m.s.:

$$x_F \equiv \frac{2p_z}{\sqrt{s}} = \frac{2p_T}{\sqrt{s}}\frac{1}{\tan\theta} = \frac{2p_T}{\sqrt{s}}\sinh(\eta). \tag{5}$$

One can see from (4) that, at least, one of the low limits $x_i^{\min}$ of the integral (3) must be $\geqslant x_F$. Thus if $x_F \geqslant 0.1$, then $x_i^{\min} > 0.1$, where the ordinary (*extrinsic*) charm distribution is completely negligible in comparison with the *intrinsic* charm distribution. Therefore, at $x_F \geqslant 0.1$, or equivalently at the charm momentum fraction $x_c > 0.1$ the *intrinsic* charm distribution intensifies the charm PDF contribution into charm hadroproduction substantially (see Fig. 1). As a result, the spectrum of the open charm hadroproduction can be increased in a certain region of p_T and η (which corresponds to $x_F \geqslant 0.1$ in accordance to (4)). We stress that this excess (or even the very possibility to observe relevant events in this region) is due to the non-zero contribution of IC component at $x_c > x_F > 0.1$ (where non-IC component completely vanishes).

This possibility was demonstrated for the D-meson production at the LHC in [15]. It was shown that the p_T spectrum of D-mesons is enhanced at pseudorapidities of $3 < \eta < 5.5$ and $10\ \text{GeV}/c < p_T < 25\ \text{GeV}/c$ due to the IC contribution, which was included using the CTEQ66c PDF [12]. For example, due to the IC PDF, with probability about 3.5%, the p_T-spectrum increases by a factor of 2 at $\eta = 4.5$. A similar effect was predicted in [30].

One expects a similar enhancement in the experimental spectra of the open bottom production due to the (hidden) intrinsic bottom (IB) in the proton, which could have a distribution very similar to the one given in (2). However, the probability w_{IB} to find the Fock state with the IB contribution $|uudb\bar{b}\rangle$ in the proton is about 10 times smaller than the IC probability w_{IC} due to relation $w_{\text{IB}}/w_{\text{IC}} \sim m_c^2/m_b^2$ [7,13].

The IC "signal" can be studied not only in the inclusive open (forward) charm hadroproduction at the LHC, but also in some other processes, such as production of real prompt photons γ or virtual ones γ^*, or Z^0-bosons (decaying into dileptons) accompanied by c-jets in the kinematics available to the ATLAS and CMS experiments. The contributions of the heavy quark states in the proton could be investigated also in the $c(b)$-jet production accompanied by the vector bosons $W^{\pm}$, Z^0. Similar kinematics given by (4) and (5) can also be applied to these hard processes.

In the next section we analyze in detail the hard process of the real photon production in pp collision at the LHC energies accompanied by the c-jet including the IC contribution in the proton.

3. Prompt photon and c-jet production

Recently the investigation of prompt photon and $c(b)$-jet production in $p\bar{p}$ collisions at $\sqrt{s} = 1.96$ TeV was carried out at the TEVATRON [17–20]. In particular, it was observed that the ratio of the experimental spectrum of the prompt photons (accompanied by the c-jets) to the relevant theoretical expectation (based on the conventional PDF which ignored the *intrinsic* charm) increases with p_T^{γ} up to factor about 3 when p_T^{γ} reaches 110 GeV/c. Furthermore, taking into account the CTEQ66c PDF, which includes the IC contribution obtained within the BHPS model [6,7] one can reduce this ratio up to 1.5 [31]. For the $\gamma + b$-jets $p\bar{p}$-production no enhancement in the p_T^{γ}-spectrum was observed at the beginning of the experiment [17,20]. However in 2012 the DØ Collaboration has confirmed observation of such an enhancement [19].

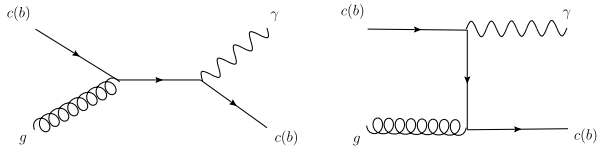

Fig. 2. The Feynman diagrams for the hard process $c(b)g \to \gamma c(b)$, the one-quark exchange in the s-channel (left) and the same in the t-channel (right).

This intriguing observation stimulates our interest to look for a similar "IC signal" in $pp \to \gamma + c(b) + X$ processes at LHC energies.

The LO QCD Feynman diagrams for the process $c(b) + g \to \gamma + c(b)$ are presented in Fig. 2. These hard sub-processes give the main contribution to the reaction $pp \to \gamma + c(b)\text{-jet} + X$.

Within LO QCD, in addition to the main subprocesses illustrated in Fig. 2 one considers the subprocesses $gg \to c\bar{c}$, $qc \to qc$, $gc \to gc$ accompanied by the bremsstrahlung $c(\bar{c}) \to c\gamma$, the contribution of which is sizable at low p_T^{γ} and can be neglected at $p_T^{\gamma} > 60$ GeV/c, according to [32]. The diagrams within the NLO QCD are more complicated than Fig. 2.

Let us illustrate qualitatively the kinematical regions where the IC component can contribute significantly to the spectrum of prompt photons produced together with a c-jet in pp collisions at the LHC. For simplicity we consider only the contribution to the reaction $pp \to \gamma + c(\text{jet}) + X$ of the diagrams given in Fig. 2. According to (5) and (4), at certain values of the transverse momentum of the photon, p_T^{γ}, and its pseudo-rapidity, η_{γ} (or rapidity y_{γ}) the momentum fraction of γ can be $x_{F\gamma} > 0.1$, therefore the fraction of the initial c-quark must also be above 0.1, where the IC contribution in the proton is enhanced (see Fig. 1). Therefore, one can expect some non-zero IC signal in the p_T^{γ} spectrum of the reaction $pp \to \gamma + c + X$ in this certain region of p_T^{γ} and y_{γ}. In principle, a similar qualitative IC effect can be visible in the production of γ^*/Z^0 decaying into dileptons accompanied by c-jets in pp collisions.

Experimentally one can measure the prompt photons accompanied by the $c(b)$-jet corresponding to the hard subprocess $c(b)g \to \gamma c(b)$ presented in Fig. 2, when γ and the $c(b)$-jet are emitted back to back. Therefore, it would be interesting to look at the contribution of this graph to the p_T^{γ} spectrum compared to total QCD calculation including the NLO corrections.

In Fig. 3 the distribution $d\sigma/dp_T^{\gamma}$ of prompt photons produced in the reaction $pp \to \gamma + c + X$ at $\sqrt{s} = 8$ TeV is presented in the interval of the photon rapidity $1.52 < |y_{\gamma}| < 2.37$ and the c-jet rapidity $|y_c| < 2.4$. The kinematic cuts used are appropriate for the ATLAS and CMS detectors [35,36]. The calculation was carried out within PYTHIA8 [33] including only graphs in Fig. 2 and the radiation corrections for the initial (ISR) and final (FSR) states along with the multi-parton interactions (MPI) within PYTHIA8.

The upper line in the top of Fig. 3 is calculated with the CTEQ66c PDF and includes IC, while the lower line uses the CTEQ66 PDF where the charm PDF is radiatively generated only. The probability of the IC contribution used is about 3.5% [12], this yields the highest sensitivity of the cross-section to the IC, however the intrinsic charm in the proton could also be about 1% [10] and therefore the results in this case will yield a lesser difference when compared to the radiatively generated ones. The ratio of the spectra with IC and without IC as a function of p_T^{γ} is presented in the bottom of Fig. 3.

One can see from Fig. 3 that the inclusion of the IC contribution increases the spectrum by a factor of 4–4.5 at $p_T^{\gamma} \simeq 400$ GeV/c, however the cross-section is too small here (about 1 fb). At $p_T^{\gamma} \simeq 150$–200 GeV/c the cross-section is about 8–30 fb

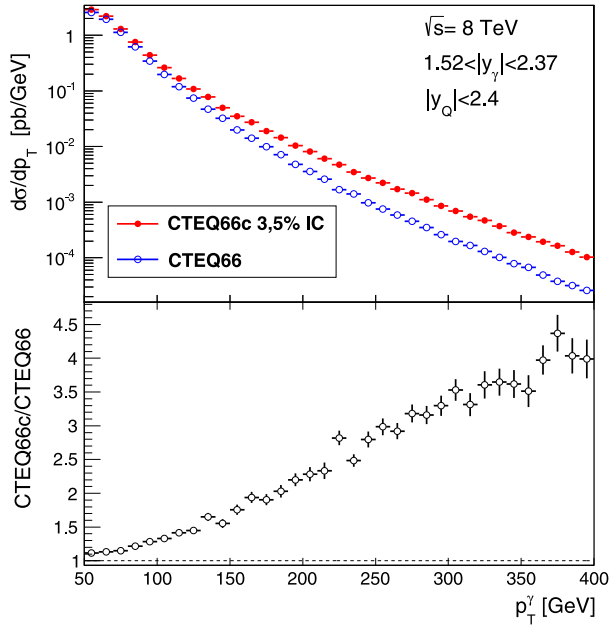

Fig. 3. The distribution $d\sigma/dp_T^\gamma$ of prompt photons produced in the reaction $pp \to \gamma cX$ over the transverse momentum p_T^γ integrated over dy in the interval $1.52 < |y_\gamma| < 2.37$, $|y_c| < 2.4$ at $\sqrt{s} = 8$ TeV. The red open points correspond to the inclusion of the IC contribution in PDF CTEQ66c with the IC probability of about 3.5% [12]; the blue solid points is our calculation using the CTEQ66 without the IC contribution in the proton. The calculation was done within PYTHIA8 using the LO QCD and including the ISR, FSR and MPI.

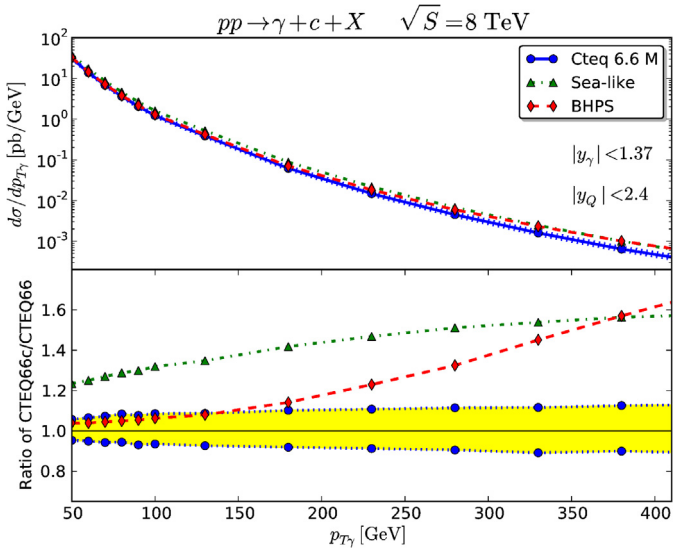

Fig. 4. The $d\sigma/dp_T^\gamma$ distribution versus the transverse momentum of the photon for the process $pp \to \gamma + c + X$ at $\sqrt{s} = 8$ TeV using CTEQ6.6M (solid blue line), BHPS CTEQ6c2 (dashed red line) and sea-like CTEQ6c4 (dash-dotted green line), for central photon rapidity $|y_\gamma| < 1.37$ (top). The ratio of these spectra with respect to the CTEQ6.6M (solid blue line) distributions (bottom). The calculation was done within the NLO QCD approximation.

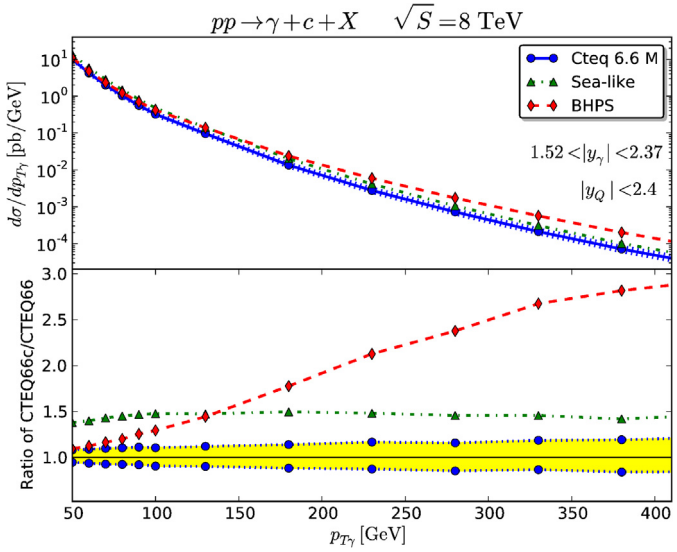

Fig. 5. The same as Fig. 4, but for forward photon rapidity $1.52 < |y_\gamma| < 2.37$.

if the IC is included and the IC signal reaches 250–300%. It corresponds to 800–3000 events in the 5 GeV/c bin for the luminosity $L = 20$ fb^{-1}. This means that even if the ATLAS/CMS c-jet reconstruction efficiency is low, there would still be plenty of statistics to make this measurement (even more so as the experimental bins are likely to be larger than the 5 GeV resolution shown here). Note that experimentally one can select the light and heavy (c and b) jets at the LHC. Some estimations of this are in progress now.

Naturally the p_T^γ distribution in Fig. 3 has the same form as the distribution over the transverse momentum of the c-quark, p_T^c, when only the hard subprocess $g + c \to \gamma + c$ in Fig. 2 is included.

In Fig. 4 the differential cross-section $d\sigma/dp_T^\gamma$ calculated at NLO in the massless quark approximation as described in [31] is presented as a function of the transverse momentum of the prompt photon. The following cuts are applied: $p_T^\gamma > 45$ GeV, $p_T^c > 20$ GeV with the c-jet pseudorapidity in the interval $|y_c| \leqslant 2.4$ and the photon pseudorapidity in the central region $|y_\gamma| < 1.37$. The solid blue line represents the differential cross-section calculated with the radiatively generated charm PDF (CTEQ66), the dash-dotted green line uses as input the sea-like PDF (CTEQ66c4) and the dashed red line the BHPS PDF (CTEQ66c2). In the lower half of Fig. 4 the above distributions normalized to the distribution acquired using the CTEQ66 PDF and $\mu_r = \mu_f = \mu_F = p_T^\gamma$, are presented. The shaded yellow region, represents the scale dependence. Clearly the difference between the spectrum using the BHPS IC PDF and the one using the radiatively generated PDF increases as p_T^γ increases.

In Fig. 5 the same distributions as in Fig. 4 are shown, however for forward photon rapidity $1.52 < |y_\gamma| < 2.37$. In this case larger x values are probed and therefore we start to observe the difference between the solid and dashed (dash-dotted) lines at smaller p_T^γ values than in Fig. 4. The difference when using the BHPS IC PDFs is about 200% at $p_T^\gamma \sim 200$ GeV. In this rapidity region the difference between the BHPS and sea-like spectra is clearly visible even as early as $p_T^\gamma \sim 200$ GeV. However, while the IC is more accentuated, the cross-section and hence the number of events is less than those for the photon central rapidity in Fig. 4.

Note that comparing Fig. 3 to Fig. 5 one can see that both the LO QCD and NLO QCD cross-section results in approximately the same IC contribution, which increases when the photon transverse momentum grows. Nevertheless the values of the spectra calculated within the NLO QCD are larger by a factor of about 1.3 than the ones obtained within the LO QCD at $p_T^\gamma > 100$ GeV/c including the ISR, FSR and the MPI. Note that all the calculations presented in Figs. 3–5 were done for the isolated photons.

Therefore Figs. 3, 5 show that the IC signal could be visible at the LHC energies with both the ATLAS and CMS detectors in the process $pp \to \gamma + c + X$ when $p_T^\gamma \simeq 150$ GeV/c. In the region the IC signal dominates over the all non-intrinsic charm background with significance at a level of a factor of 2 (in fact 170%).

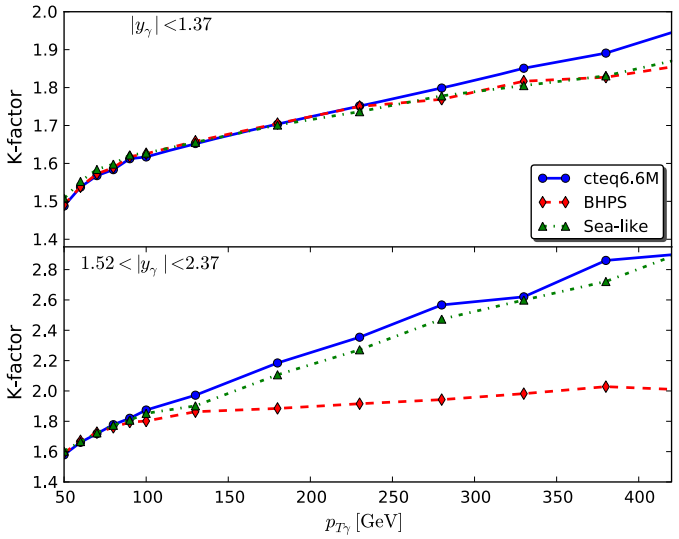

Fig. 6. The so-called QCD K-factor, or the ratio of the NLO contribution to the LO one, for the central photon rapidity region $|y_\gamma| < 1.37$ (top), and the forward photon rapidity $1.52 < |y_\gamma| < 2.37$ (bottom).

In Fig. 6 the K-factor, or the ratio between the NLO and LO contributions to the photon and charm jet cross-section, for the central and forward rapidity regions is presented showing the dependence of the different initial state PDFs. It is clear that the K-factor using the BHPS PDF at $p_T\gamma$ ranges where the x is large is much smaller with respect to the one using the radiatively generated charm PDF. The dependence on the heavy quark PDF is felt in the LO Compton subprocess ($gQ \to \gamma Q$), whose contribution increases. At NLO it is the higher order correction, $gQ \to gQ\gamma$ to the Compton subprocess that dominates the cross-section [34], which also increases when using the BHPS PDF, while the rest of the NLO contributions not dependent on the heavy quark PDF remain the same. This increase in the LO with respect to the NLO when using the BHPS PDFs causes the K-factor for the BHPS to decrease, at high p_T, as well as in particular in the forward rapidity range, where an even higher x is probed.

4. Conclusion

In this Letter we have shown that the possible existence of the intrinsic heavy quark components in the proton can be seen not only in the forward open heavy flavor production in pp-collisions (as it was believed before) but it can be visible also in the semi-inclusive pp-production of prompt photons and c-jets at rapidities $1.5 < |y_\gamma| < 2.4$, $|y_c| < 2.4$ and large transverse momenta of photons and jets. In the inclusive photon spectrum measured together with a c-jet a rather visible enhancement can appear due to the intrinsic charm (IC) quark contribution. In particular, it was shown that the IC contribution can produce much more events (factor 2 or 3) at $p_T^\gamma > 150$ GeV/c and forward y_γ in comparison with the relevant number expected in the absence of the IC. Furthermore the same enhancement is also coherently expected in the transverse momentum, p_T^c, distribution of the c-jet measured together with the above-mentioned prompt photon in the $pp \to \gamma + c\text{-jet} + X$ process.

Searching for the signal of *intrinsic* charm in such processes is more pronounced than the search for the *intrinsic* bottom because the IB probability is, at least, in 10 times smaller than the IC probability in the proton.

Experimentally, measuring this channel will be complicated due to the light and bottom quark backgrounds, but with such a large difference between models it should still be visible in the kinematic ranges suggested here.

Acknowledgements

We thank S.J. Brodsky and A.A. Glasov for extremely helpful discussions and recommendations by the study of this topic. The authors are grateful to H. Jung, A.V. Lipatov, V.A.M. Radescu, A. Sarkar and N.P. Zotov for very useful discussions and comments. This research was also supported by the RFBR grants No. 11-02-01538-a and No. 13-02001060.

References

[1] J.W. Negele, et al., Nucl. Phys. B, Proc. Suppl. 128 (2004) 170; W. Schroers, Nucl. Phys. A 755 (2005) 333.
[2] V.N. Gribov, L.N. Lipatov, Sov. J. Nucl. Phys. 15 (1972) 438; G. Altarelli, G. Parisi, Nucl. Phys. B 126 (1997) 298; Yu.L. Dokshitzer, Sov. Phys. JETP 46 (1977) 641.
[3] J. Pumplin, D.R. Stump, J. Huston, H.L. Lai, P. Nadolsky, W.K. Tung, J. High Energy Phys. 0207 (2002) 012; D.R. Stump, J. Huston, J. Pumplin, W.K. Tung, H.L. Lai, S. Kuhlmann, J.F. Owens, J. High Energy Phys. 0310 (2003) 046.
[4] R.S. Thorne, A.D. Martin, W.J. Stirling, R.G. Roberts, arXiv:hep-ph/0407311.
[5] A. Aktas, et al., H1 Collaboration, Eur. Phys. J. C 40 (2005) 349, arXiv:hep-ex/0507081.
[6] S. Brodsky, P. Hoyer, C. Peterson, N. Sakai, Phys. Lett. B 93 (1980) 451.
[7] S. Brodsky, C. Peterson, N. Sakai, Phys. Rev. D 23 (1981) 2745.
[8] J.F. Donoghue, E. Golowich, Phys. Rev. D 15 (1977) 3421.
[9] J. Pumplin, Phys. Rev. D 73 (2006) 114015.
[10] J. Pumplin, H.L. Lai, W.K. Tung, Phys. Rev. D 75 (2007) 054029.
[11] Jen-Chien Peng, Wen-Chen Chang, in: Sixth Intern. Conf. on Quarks and Nuclear Physics, Ecole Polytechnique Palaiseau, Paris, April 16–20, 2012, arXiv:1207.2193 [hep-ph].
[12] P.M. Nadolsky, et al., Phys. Rev. D 78 (2008) 013004.
[13] M.V. Polyakov, A. Schafer, O.V. Teryaev, Phys. Rev. D 60 (1999) 051502.
[14] V. Goncalves, F. Navarra, Nucl. Phys. A 842 (2010) 59.
[15] G.I. Lykasov, V.A. Bednyakov, A.F. Pikelner, N.I. Zimin, Europhys. Lett. 99 (2012) 21002, arXiv:1205.1131v2 [hep-ph].
[16] V.A. Litvine, A.K. Likhoded, Phys. At. Nucl. 62 (1999) 679.
[17] V.M. Abazov, et al., Phys. Rev. Lett. 102 (2009) 192002, arXiv:0901.0739 [hep-ex].
[18] V.M. Abazov, et al., Phys. Lett. B 719 (2013) 354, arXiv:1210.5033 [hep-ex].
[19] V.M. Abazov, et al., Phys. Lett. B 714 (2012) 32, arXiv:1203.5865 [hep-ex].
[20] T. Aaltonen, et al., Phys. Rev. D 81 (2010) 052006, arXiv:0912.3453 [hep-ex].
[21] R. Vogt, Prog. Part. Nucl. Phys. 45 (2000) S105.
[22] F.S. Navarra, M. Nielsen, C.A.A. Nunes, M. Teixeira, Phys. Rev. D 54 (1996) 842.
[23] W. Melnichouk, A.W. Thomas, Phys. Lett. B 414 (1997) 134.
[24] A.V. Efremov, Sov. J. Nucl. Phys. 19 (1974) 176.
[25] P. Nasson, S. Dawson, R.K. Ellis, Nucl. Phys. B 327 (1989) 49.
[26] R.D. Field, R.P. Feyman, Phys. Rev. D 15 (1977) 2590.
[27] R.P. Feyman, R.D. Field, G.C. Fox, Phys. Rev. D 18 (1977) 3320.
[28] M.L. Mangano, Phys. Usp. 53 (2010) 109.
[29] S. Albino, B.A. Kniehl, G. Kramer, AKK08, Nucl. Phys. B 803 (2008) 42.
[30] B. Kniehl, G. Kramer, I. Schienbein, H. Spiesberger, Eur. Phys. J. C 72 (2012) 2082, arXiv:1202.0439v1 [hep-ph].
[31] T.P. Stavreva, J.F. Owens, Phys. Rev. D 79 (2009) 054017, arXiv:0901.3791 [hep-ph].
[32] A.V. Lipatov, M.A. Malyshev, N.P. Zotov, J. High Energy Phys. 1205 (2012) 104, arXiv:1204.3828 [hep-ph].
[33] T. Sjostrand, S. Mrenna, P.Z. Skands, Comput. Phys. Commun. 178 (2008) 852.
[34] T. Stavreva, et al., J. High Energy Phys. 1101 (2011) 152, arXiv:1012.1178 [hep-ph].
[35] ATLAS Collaboration, J. Instrum. 3 (2008) S08003.
[36] CMS Collaboration, J. Instrum. 3 (2008) S08004.